Report

Current Biology

Consistency of Spatial Representations in Rat Entorhinal Cortex Predicts Performance in a Reorientation Task

Highlights

- Entorhinal grid and head-direction maps show remarkable stability
- Disorientation occasionally leads to rotation of these maps
- Behavior does not influence the rotation of entorhinal maps
- Use of entorhinal maps for wayfinding is dependent on memory of signal reliability

Authors

Shahaf Weiss, Ghadeer Talhami, Xenia Gofman-Regev, Sophia Rapoport, David Eilam, Dori Derdikman

Correspondence

shahaf.me@gmail.com (S.W.), derdik@technion.ac.il (D.D.)

In Brief

Using a variation of the reorientation task, Weiss et al. find a role for the stability of orientation signals in the entorhinal cortex of rats. Alignment and stability of past and present representations predict corner choice and highlight the connection between reliability of the neuronal signal and behavioral decisions.

Weiss et al., 2017, Current Biology *27*, 3658–3665
December 4, 2017
https://doi.org/10.1016/j.cub.2017.10.015

CellPress

CellPress

Current Biology
Report

Consistency of Spatial Representations in Rat Entorhinal Cortex Predicts Performance in a Reorientation Task

Shahaf Weiss,[1,2,*] Ghadeer Talhami,[1] Xenia Gofman-Regev,[1] Sophia Rapoport,[1] David Eilam,[2] and Dori Derdikman[1,3,*]
[1]Department of Neuroscience, Rappaport Faculty of Medicine and Research Institute, Technion – Israel Institute of Technology, Haifa 31096, Israel
[2]School of Zoology, George Wise Faculty of Life Sciences, Tel Aviv University, Ramat-Aviv 69978, Israel
[3]Lead Contact
*Correspondence: shahaf.me@gmail.com (S.W.), derdik@technion.ac.il (D.D.)
https://doi.org/10.1016/j.cub.2017.10.015

SUMMARY

Goal-directed behavior can be affected by environmental geometry. A classic example is the rectangular arena reorientation task, where subjects commonly confuse opposite but geometrically identical corners [1]. Until recently, little was known about how environmental geometry shapes spatial representations in a neurobehavioral context [2] (although see [3]). In the present study, we asked: Under what circumstances does the internal cognitive map predict behavior? And when does it fail to do so? To this end, we developed a variant of the classical reorientation task that allows for investigation of temporal dynamics of reorientation. We recorded head-direction (HD) cells and grid cells in the medial entorhinal cortex (MEC) of rats before, during, and after performing the task. MEC cells showed a bimodal response of being either aligned or rotated, relative to the free-foraging open-field sessions. Alignment was remarkably stable between disorientations and indicative of corner choice as a function of current and past alignment of spatial representations. Accordingly, when the cells showed consistent and properly aligned readout across multiple trials, behavioral choices were better predicted by HD and grid cell readout, with a probability of more than 70%. This was not the case when the cells did not show a stable consistent readout. Our findings indicate that entorhinal spatial representations predict corner choice, contingent on the stability and reliability of their readout. This work sets the stage for further studies on the link between the reliability of the neuronal signal and behavior, with implications for many brain systems in many organisms.

RESULTS AND DISCUSSION

Despite the abundance of spatially correlated neural activity patterns in the hippocampal formation [4–11], little is known about how medial entorhinal cortex (MEC) internal maps are modulated by external inputs and the impact of such modulations on behavior. In an effort to understand the relationship between activity patterns of spatially selective cells and behavior in a task, we employed a classical reorientation task [1]. The task involved training a rat to seek a food reward in one corner of a rectangular arena; rotating the rat, causing disorientation; and tracking the first corner in which the rat then searched for the reward. Rats often confused between the correct corner and the opposite, geometrically identical corner, known as a "rotational error." Similar behavior was found in many species [12–21]. In the current study, we examined whether the behavior in the reorientation task was dependent on entorhinal cells, that is, if animals were able to rely on past experiences. A custom variant of the classical reorientation task enabled us to explore the temporal dynamics of entorhinal spatial maps during recovery from disorientation across extended timescales by distinguishing trials after disorientation events from recent yet oriented trials. We recorded head-direction (HD) cells and grid cells in the MEC of five rats (Figure 1A). Rats were trained to perform a spatial reorientation task in a 60 × 120 × 60 cm arena, with externally controllable feeders at the arena corners and a central spinning plate (Figure 1B). All trials began and ended with the rat inside the central plate, confined by a collapsible polyvinyl chloride (PVC) cylinder. An A-B-A' experimental design was used (Figure 1C) to identify spatially selective cells and to examine the stability of the recorded cells across all sessions. The first and last sessions in a recording day (A and A') comprised an open-field random foraging task, in which rats foraged for randomly distributed chocolate sprinkles. The intermediate session (B) consisted of the reorientation task, in which rats were rewarded at a single corner of the arena and were periodically disoriented. We note that A, B, and A' were separate recording sessions, with several hours between them. Only B contained the reorientation task, whereas A and A' were free-foraging sessions used to characterize the spatial selectivity of the recorded HD cells and grid cells, as described below. The task (B) comprised blocks of multiple trials; at each trial, the rat ran from the center to find the reward and then back to the center. The first trial of each block, except for the first block, was preceded by disorientation of the rat (Figure 1C).

We first quantified the behavior of the rat in the reorientation task. Task sessions consisted of 2–10 blocks of trials, separated by disorientation events (Figure 1D). Each block contained 6–8

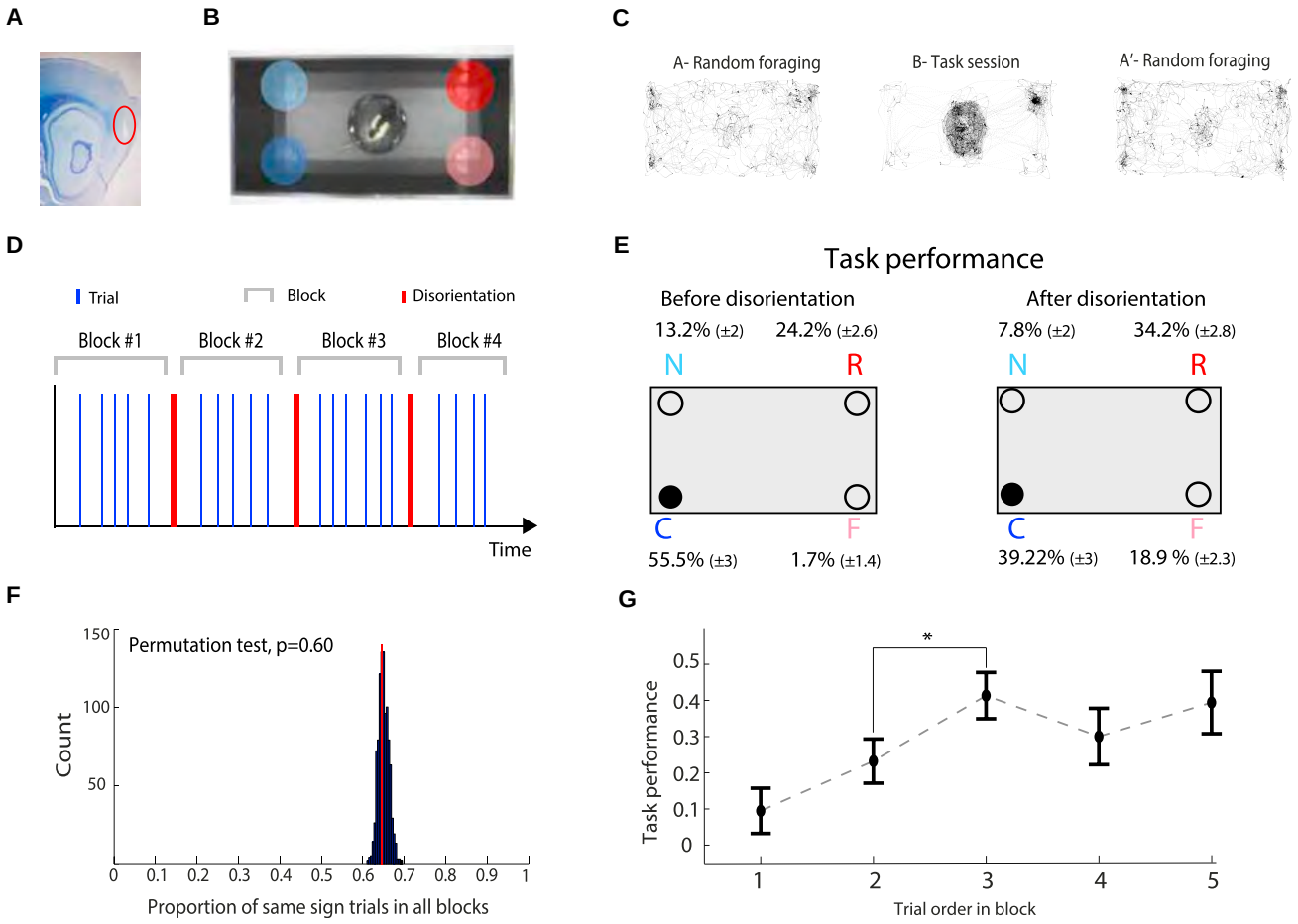

Figure 1. Experimental Design and Behavioral Results

(A) Histological preparation. Tetrode trace in MEC is shown (red circle).

(B) Layout of apparatus. Example of corner choices for a single recording day is shown (the correct corner location was changed between recording days), color-coded for illustration purposes—blue for correct choice, light blue for near error, light red for far error, and red for rotational error.

(C) A typical example of a trajectory in A, first open-field recording; B, task session; and A', second open-field recording.

(D) Schematic representation of a reorientation task session.

(E) Ratios of task performance scores for different corner choices. The chance level for choice among four corners is 25%. C, correct; F, far error; N, near error; R, rotational error. Before disorientation, there was a clear difference between correct and rotational choice ratios as noted above; following disorientation, there was no significant difference between both corner choices (H_0: equal ratios between correct and rotational corner choices; $\chi^2 = 0.4763$; df = 1; p = 0.49). The ratio of geometrically identical corner choices (correct and rotational) versus non-geometrically identical corner choices (near and far) did not differ significantly before and after disorientation ($\chi^2 = 3.208$; df = 1; p = 0.073). However, this ratio was significantly different from a null hypothesis stating that corner choice was not affected by geometry (H_0: equal ratios between geometrically identical versus non-identical corners; $\chi^2 = 31.827$; df = 1; p < 0.0001). Similar findings were obtained for task engagement parameters (Figure S1B).

(F) The stability of behavioral outcomes within trial blocks. Blue bars, population of 1,000 permutated trials; red line, the observed proportion of same sign trials (positive or negative performance scores).

(G) The position-triggered mean task performance scores for all trial blocks (mean ± SEM) considering only correct and rotational choices.

*p < 0.05. Within blocks, the mean task performance improved from 0.23 ± 0.06 in the second trial to 0.41 ± 0.08 in the third trial (Wilcoxon signed-rank test; z = −2.08; p < 0.05). See also Figures S1 and S2.

trials between disorientations (except for one rat, which had 2–8 trials in each block). Variability in the number of trials and blocks was related to the rat's performance—the experimenter had to balance between too many disorientations and not enough disorientations while maintaining the rat's engagement in the task at a high level. Too many disorientations caused some rats to stop "playing the game" and not initiate new trials. The experimental setup depended on active initiation of trials by the rats, and thus variability was required for the rats' good performance.

We employed two behavioral classifiers (see STAR Methods): the main behavioral classifier measured task performance, revealing the rat's first choice. An additional behavioral classifier measured task engagement, revealing the level of engagement of the animals in performing the task (Figure S1A). We note that the behavioral classifier we used for task performance was related to the rat's first "automatic" darting out once the cylinder was removed. This is different from the classical classifier used in previous reorientation experiments by Cheng and

colleagues [1, 12–22] and was chosen due to differences between our variant of the task and the original task.

We graded each corner choice with a numerical value: +1 for a correct choice and −1 for a rotational error choice. Near and far error choices were omitted from the analysis, in line with previous studies that compared mostly correct and rotational error behaviors and as the latter composed the majority of behavioral choices (Figure 1E). We set out to characterize the effects of spin-induced disorientation on the behavioral outcome of trials and trial blocks. In accordance with previous behavioral studies [1, 21], in trials that preceded disorientation, rats achieved more correct choices, on average, than rotational errors: 56% (n = 156) versus 24% (n = 68). Following disorientation, the proportion of correct choices was 39% (n = 110), whereas the proportion of rotational error choices was 34% (n = 96; Figure 1E). We found a significant difference in corner choice ratios before and after disorientation for both the general distribution of all corner choices (χ^2 = 19.119; df = 3; $p < 0.001$) and for a subset that was limited to the correct corner and rotational error choices (χ^2 = 12.003; df = 1; $p < 0.001$). Overall, our behavioral results were similar to those reported in Cheng [1], although, as we noted above, our task differed in several aspects from the original task so that it would be better adapted to our electrophysiological recordings. We measured the stability of behavioral choices within blocks by comparing the ratio of correct versus rotational behavioral choices within the same block as an estimate of performance. We found that neither behavioral classifier showed significant stability of correct/rotational trial ratios within blocks (permutation test; $p = 0.60$ for task performance; see STAR Methods; Figure 1F). A learning curve emerged regarding the behavioral performance of rats within blocks (Figure 1G). Following initial disorientation, performance of the task recovered within three trials. We acknowledge that the improved performance along the block may be due to the study design, which allowed the rat to search for the correct corner after initial failure. This practice was afforded to maintain the animal's motivation during long recording sessions, up to an hour and a half, and to provide enough sampling during a trial to determine the coding of the HD cell or grid cell, though note that performance along the trials of a block did not reach values higher than 0.5, even in late trials. This is because performance was quite random after disorientation and seemed to remain that way also in later trials in the block. For this reason, we only included task sessions with complete coverage of all corners in our analysis, yet complete coverage could not be attained in each and every trial.

We sought to determine the response of the cells to disorientation. Single-cell temporal activity patterns of HD cells revealed a typical orientation for each cell in each trial. In single-cell examples, at the beginning of the task, HD cells and grid cells retained their open-field orientations. Cells occasionally shifted their preferred firing direction (PFD) in trials that followed disorientation episodes but tended to remain stable within behavioral blocks. The magnitude of the shifts in the PFD of HD cells was not random but was often distributed around two distinct values, roughly 180° apart: one was similar to the PFD observed in an open-field random foraging session in the same environment and the other was 180° away from the open field (Figure 2A). To normalize for different PFDs of multiple simultaneously recorded HD cells, we defined an HD orientation score. When the PFD was totally aligned to the open field, its value was 1, whereas, when the PFD was rotated by 180° relative to the open field, its value was −1 (see STAR Methods for normalization formula). For grid cells, we defined a grid orientation score as equal to 1 when the grid pattern in a trial was congruent with the open field and as equal to −1 when the grid pattern was congruent with the 180° rotated open field (see STAR Methods). In single cells, rate maps generated for each block typically displayed similarity to those of open-field recordings or to a 180° rotated version of the same recordings (Figure 2B).

Population vectors of HD and grid orientation scores were calculated for each session as the average scores for the trial across all simultaneously recorded cells for each cell type. Both population vectors showed stable response patterns within trial blocks. Following disorientation events, ensembles of HD cells or grid cells tended to remain either in the same orientation or to shift their orientation together as an ensemble (Figures 2C and 2D).

Unlike behavior, HD and grid orientation scores were strikingly stable within each block, such that typically, either positive or negative orientation scores were observed consistently throughout trials within a single block. The orientation score of population vectors was found to be significantly more stable than expected, for both HD cells and grid cells (permutation test; $p < 0.01$ for both; Figures 2E and 2F). Stability was not dependent on the number of trials in a block (Figures S2C and S2D). This result indicates that the HD and grid population vectors tended to shift around disorientation events, but not within trial blocks. In other words, HD and grid population orientation was either similar to the open-field recording or rotated by 180° throughout all the trials of a single block. We concluded that the HD cells were markedly stable within each trial block, shifting in most cases by 180° and only after disorientation events.

Population vector scores of HD cells and grid cells that were recorded simultaneously were found to be significantly correlated (Spearman correlation; $r = 0.38$; $p = 1.4 \times 10^{-37}$; n = 1,058 trials; Figure 3A), and the correlation was maintained in an analysis that included only trials that immediately followed disorientation events (Spearman correlation; $r = 0.45$; $p = 1.96 \times 10^{-14}$; n = 240 trials; containing both HD and grid population vector scores; Figure 3B). The high degree of coordination between HD cells and grid cells was also evident on single experimental days (Figure 3C). Taken together, these results indicate that, remarkably unlike behavior, HD and grid population vectors retained their orientation during behavioral blocks but occasionally shifted their orientation following disorientation events.

Next, we set out to determine relationships among HD population responses, grid population responses, and behavioral performance. We thus sought to assess whether orientation states and state transitions of the HD and grid population vectors predicted behavior. We calculated the probabilities of corner choices in the first trial after the disorientation, given the HD or grid population vectors in this and previous trials (Figures 4A–4D). Considering the current trial only, the probability of a correct choice over a rotational error following a disorientation event was 0.57, given a positive orientation score for HD cells (Figures 4A and 4B) or 0.61 for grid cells (Figures 4C and 4D; the chance level was 0.50). If the HD population vector in a previous trial was properly aligned, the probability of a correct choice significantly increased from 0.57 to 0.65; however, if the

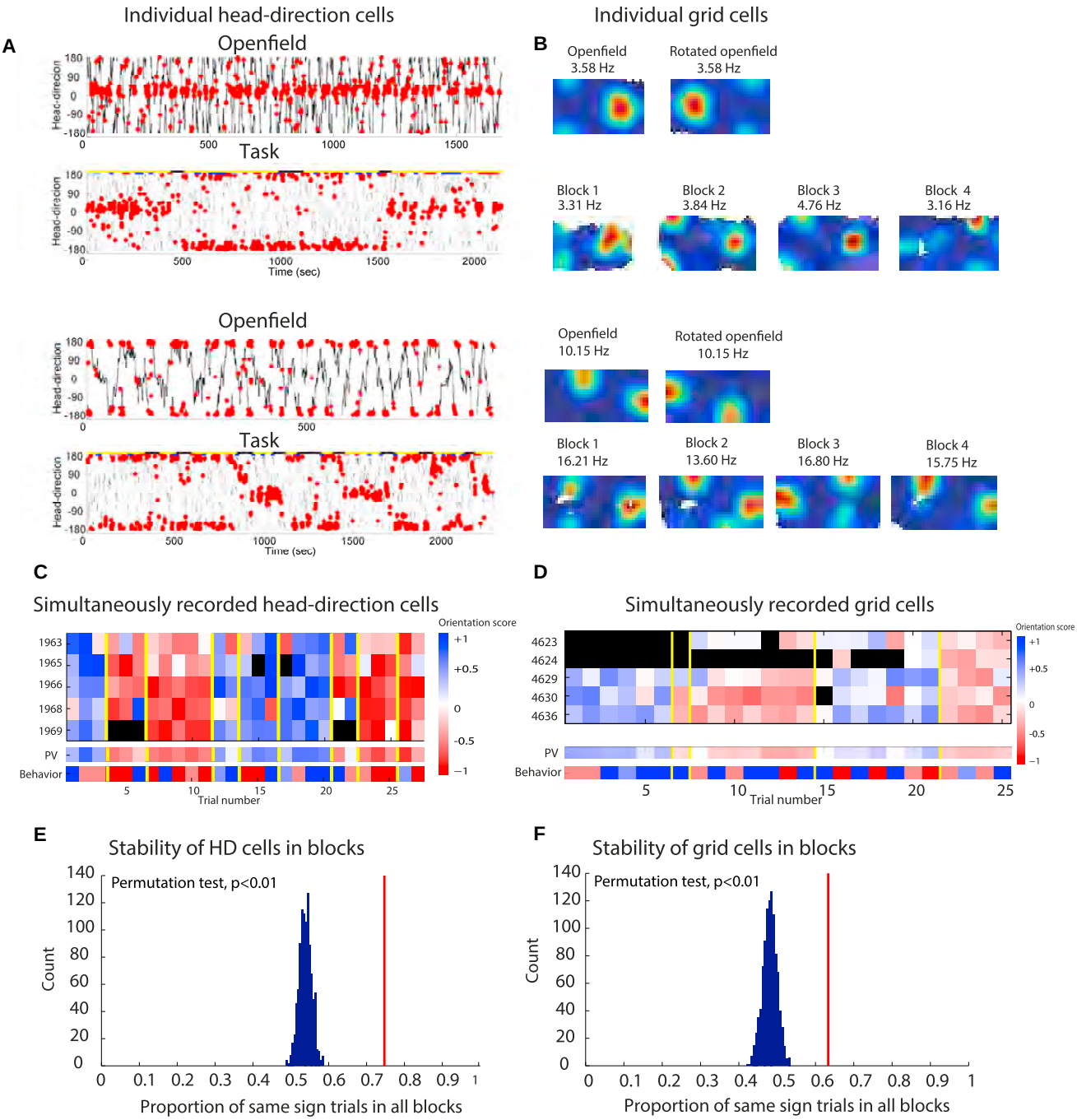

Figure 2. Response of HD Cells and Grid Cells to Disorientation

(A and B) Examples of head-direction (HD) cell and grid cell activity during open-field versus task sessions. (A) Responses of two HD cells are shown. Each panel depicts HD (black) over time and HD during spike times (red) in a random foraging session versus a task session. The bottom part of each panel depicts the HD and spike times during the reorientation task. Black horizontal bars indicate periods of disorientation epochs. Yellow bars indicate periods between disorientation episodes. Blue bars indicate correct trials, light-blue bars indicate near error trials, red bars indicate rotational error trials, and light-red bars indicate far error trials. (B) Rate maps of two grid cells are shown. Top and third rows, rate map of open-field, random foraging session, and a 180° rotated version of the same rate map; second and fourth rows, rate maps of four trial blocks, showing rotation of the grid between blocks while maintaining the overall grid structure.

(C and D) Visualization of orientation scores in the task for simultaneously recorded HD cells (C) and grid cells (D). Each square represents a single trial, color coded according to the HD orientation score observed during that trial. Scores are scaled from +1 (blue) to −1 (red); trials in which the firing rate was under 0.05 Hz are marked in black. Yellow lines represent disorientation events between trials. Population vector and task scores for corresponding trials are displayed below each panel.

(E and F) The stability of orientation scores for HD (E) and grid cells (F) within blocks. The observed proportion of same sign trials (red line) versus 1,000 permutations of trials from different blocks (blue bars) is shown.

See also Figures S1, S2, and S4.

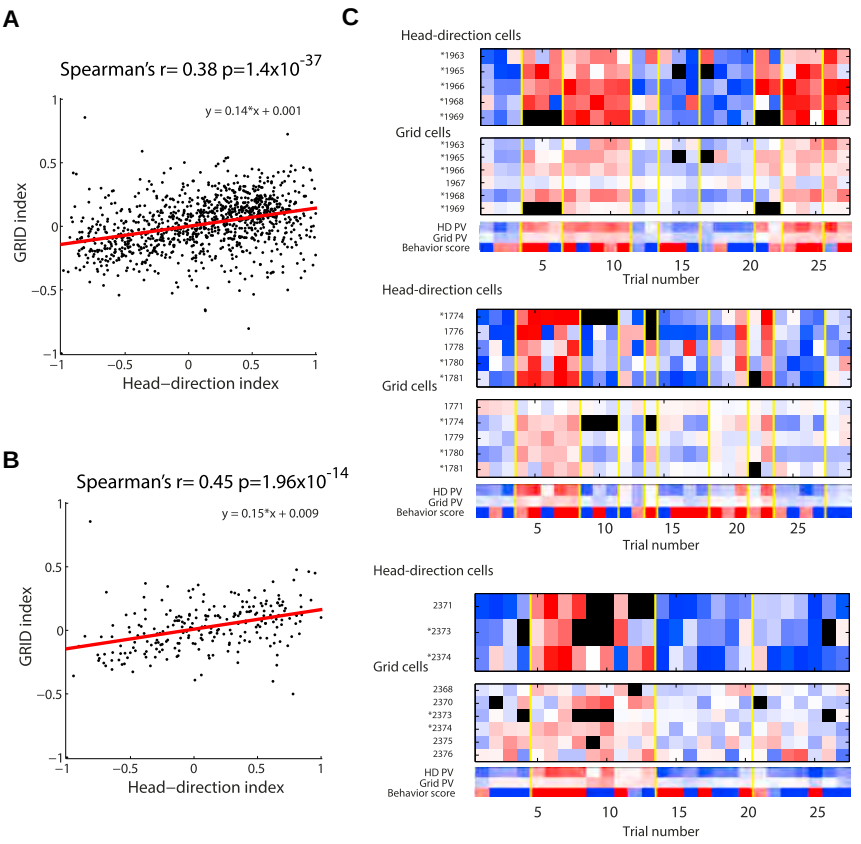

Figure 3. Simultaneously Recorded HD Cells and Grid Cells Share Orientation of Alignment

(A) HD scores and grid orientation population vector scores for all trials with simultaneously recorded cells of both types.

(B) Same as (A) but only for trials immediately following disorientation events.

(C) Trial-by-trial visualization of HD and grid orientation scores during three recording sessions (asterisks mark conjunctive HD × grid cells) for simultaneously recorded cells. Scores are scaled from +1 (blue) to −1 (red). Trials in which the firing rate was under 0.05 Hz are marked in black. Yellow vertical lines represent disorientation events between trials.

See also Figures S1, S2, and S4.

HD population vector in the previous trial (before disorientation) was misaligned (n = 65; 33 instances; $\chi^2 = 9.48$; df = 2; $p < 0.01$), the probability dropped to 0.42. Proper alignment in 2 previous trials increased the probability of a correct choice to 0.68, whereas misalignment decreased the probability to 0.29 (n = 39; 12 instances; $\chi^2 = 7.41$; df = 2; $p < 0.05$) and subsequently to 0.69 versus 0.25, respectively, for 3 previous trials (n = 53; 21 instances; $\chi^2 = 6.24$; df = 2; $p < 0.05$). These differences were also maintained in an analysis that considered 4–6 previous trials (Figure 4A). The results for grid cells were less dramatic than for HD but showed a similar trend (Figure 4C). These results suggest that the behavioral response was dependent on the reliability of the HD or grid signal in previous trials. Similar results were achieved when analyzing whole blocks instead of trials (Figures S3A–S3D).

The above findings reflect a process by which, on one hand, the rats could increasingly rely on the reading of HD cells (with similar trends in grid cells) for performance of the task, contingent on HD cells being properly aligned in past blocks, whereas, on the other hand, they did not rely on these cells when they were incorrectly aligned.

Our results show that, during the reorientation task, HD cells and grid cells were significantly stable between disorientation events (within trial blocks) and that they changed only after rotation of the animal. In addition, the orientation of these cells was either aligned to, or pointing away from, the orientation recorded in a random foraging task in the same arena. Simultaneously recorded HD cells and grid cells tended to shift as a single cohort, promoting the use of cell population vectors as indicators of cell ensemble activity. Grid cells demonstrated a similar relationship to behavior as HD cells and were also coordinated to the activity of the HD cells in respect to reorientation. Whereas the behavior fluctuated, the HD and grid cells were very stable between disorientations. We found that activity of these cells predicted behavior mostly in cases where correct alignment was maintained for several trials. Otherwise, if alignment was recently flipped, the rat did not rely on the readout from these cells for behavior.

We focused our analysis on internal representation and its prediction of behavior. However, we did not deal here with the rat's behavioral strategy as manifested, for example, by the addition of local features, because this was addressed in many previous works [1, 3, 23–28]. A recent study of hippocampal CA1 place cells in mice [3] showed that, in a reorientation task, the alignment of hippocampal maps to the geometric axes in the environment was related to search behavior within a trial. In the current study, entorhinal cells displayed an experience-dependent relationship between search behavior and neural representation of position and heading in the MEC. Thus, as noted above, the dependence of behavior on the HD signal was related to the consistency or reliability of the latter in memory. A possible explanation for the discrepancy in neural readouts of a similar behavioral task lies in the dissimilarities of experimental design. As such, whereas the task employed in [3] was essentially a reference memory task, the task in the current study was a more complex block design, which could be interpreted as a working memory task. Our design offers insight into the slower temporal dynamics of the internal cognitive map during recovery from disorientation. We were thereby able to scrutinize the effect of continuous alignment of entorhinal spatial representations and behavioral choice in the task. When proper alignment was not maintained, we suggest that the rats relied on other navigational systems to find the reward location. Specifically, parallel orientation systems continuously compete for dominance to accurately guide the rat to its goal, mainly the hippocampal allocentric navigational system and the striatal egocentric system or another compensatory neural system,

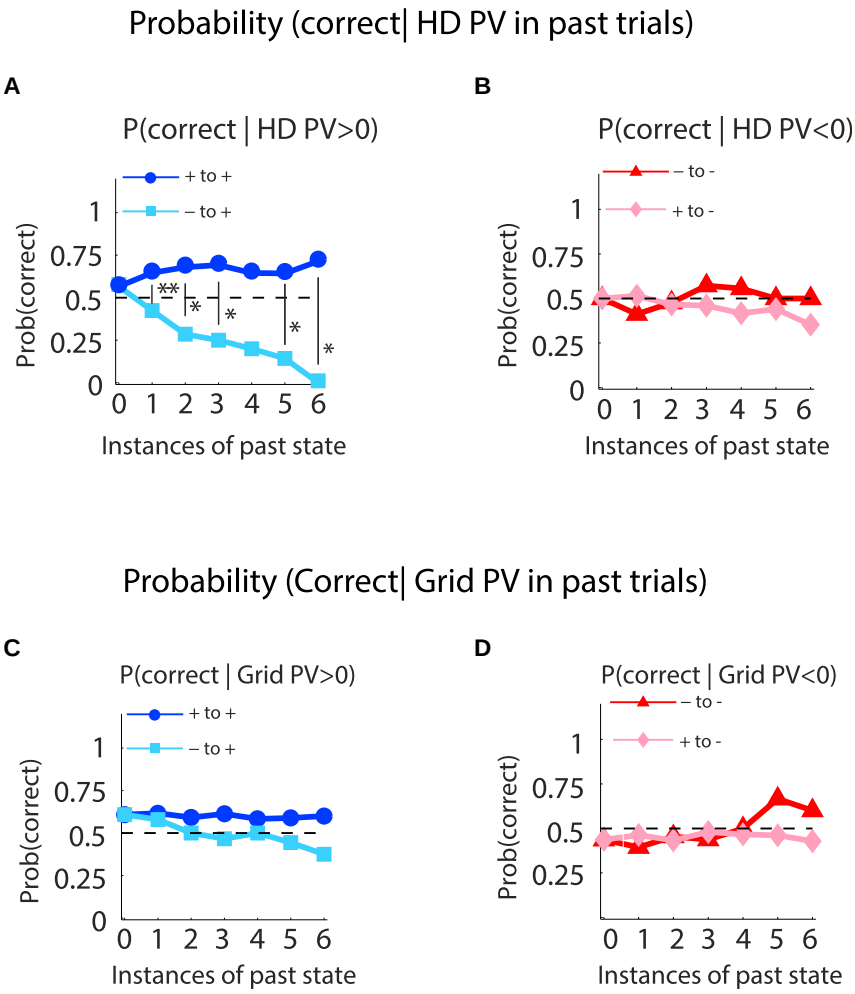

Figure 4. The Probability of a Behavioral Outcome Depends on Current and Past Trial Population Vectors of HD or Grid Orientation Scores

An increase in probability for correct corner choice was found in cases of properly aligned HD or grid representations over multiple trials. For each data point, the probability of choice was compared to the probability observed without considering population vectors from previous trials. See also Figures S1–S3.

(A) The probability of a correct corner choice, given a positive HD population vector in the current trial, and a positive (blue) or negative (cyan) population vector in the previous n trials ("instances of past state"). *$p < 0.05$; **$p < 0.01$.

(B) The probability of a correct corner choice, given a negative HD population vector in the current trial, and a negative (red) or positive (pink) population vector in the previous n trials.

(C) The probability of a correct corner choice, given a positive grid population vector in the current trial. Color code is similar to (A).

(D) The probability of a correct corner choice, given a negative grid population vector in the current trial. Color code is similar to (B).

such as the posterior parietal cortex. These systems can at times contain contradictory information [29–34]. A recent model of reorientation tasks in humans [35] proposed that information regarding the target location can be derived by adaptively combining cues used by different memory systems, according to available information (geometrical, associative, and polarizing cues). Similarly, our study highlights the relationship of behavior to such parallel memory systems. This suggests that the use of the entorhinal spatial map for wayfinding depends on the reliability and consistency of its readout.

Previous studies have correlated the accumulation of errors in HD cells recorded in anterodorsal thalamic nucleus (ADN) and dorsal presubiculum (dPRS) with heading errors in path integration tasks in both passive and active disruption of the HD system [36–38] or the ability of HD cells to track rotation of a cue with arm choice in a radial maze [39]. In contrast, ADN cells recorded in a reorientation task did not show a clear correlation with behavioral choices [2]. In the same vein, our results emphasize the importance of accurate alignment of internal maps to external cues as a predictor of behavioral performance and the role of signal stability in orientation in a behavioral context; the latter was previously unexplored. Our results demonstrate that the use of entorhinal spatial maps for wayfinding is dependent on signal reliability, whereas different timescales exist for the internal cognitive map versus behavioral output. In a broader perspective, our results demonstrate that the HD (and grid) memory system, being a continuous and persistent signal [40], helps guide the behavior of rats according to their recent experience, based on consistency to stored representations [41]. Our results have important implications for understanding how the brain controls behavior—it is a demonstration that the influence of a certain brain system on behavior (in this case, the entorhinal map) is dependent on how reliable this system was in the near past in helping to fulfill the task and getting the reward. In other words, if a system was unreliable in achieving the reward, it stops dictating behavior. This finding can potentially apply to principal mechanisms for controlling behavior and extend beyond rodent spatial behavior. We hope our results will attract further research into the role of neuronal signal stability in determination of behavior and promote further discussion, as there are very few studies to date that tackle the important question of the relation between the cognitive map and behavior.

STAR★METHODS

Detailed methods are provided in the online version of this paper and include the following:

- KEY RESOURCES TABLE
- CONTACT FOR REAGENT AND RESOURCE SHARING
- EXPERIMENTAL MODEL AND SUBJECT DETAILS
  - Subjects and surgery

SUPPLEMENTAL INFORMATION

Supplemental Information includes four figures and can be found with this article online at https://doi.org/10.1016/j.cub.2017.10.015.

AUTHOR CONTRIBUTIONS

Conceptualization, S.W., D.D., and D.E.; Methodology, S.W. and D.D.; Software, S.W. and D.D.; Investigation, S.W., G.T., S.R., and X.G.-R.; Resources, D.D. and D.E.; Data Curation, S.W.; Writing – Original Draft, S.W. and D.D.; Writing – Review & Editing, S.W., D.D., and D.E.; Visualization, S.W.; Supervision, D.D.; Funding Acquisition, D.D. and D.E.

ACKNOWLEDGMENTS

We thank Genela Morris for critical reading of the manuscript and Naomi Paz and Cindy Cohen for proofreading. We thank the Pathology Department in the Rambam Health Care Campus and Asya Rolls and her lab for assistance with histology. We thank Chen Elbak for help with experiment administration. We thank members of the Derdikman lab, and especially Gilad Tocker, for ongoing technical assistance and discussions and Ohad Rechnitz for help with microdrive manufacturing. This research was supported by the Israel Science Foundation (personal grants 955/13 and 2344/16 and equipment grant 1882/13 to D.D. and personal grant 230/13 to D.E.), by a Rappaport Institute grant (to D.D.), by an Allen and Jewel Prince Center for Neurodegenerative Disorders of the Brain grant (to D.D.), and by the Adelis Foundation - joint Technion and Weizmann program (to D.D.).

Received: June 25, 2017
Revised: September 17, 2017
Accepted: October 5, 2017
Published: November 16, 2017

REFERENCES

1. Cheng, K. (1986). A purely geometric module in the rat's spatial representation. Cognition *23*, 149–178.
2. Golob, E.J., Stackman, R.W., Wong, A.C., and Taube, J.S. (2001). On the behavioral significance of head direction cells: neural and behavioral dynamics during spatial memory tasks. Behav. Neurosci. *115*, 285–304.
3. Keinath, A.T., Julian, J.B., Epstein, R.A., and Muzzio, I.A. (2017). Environmental geometry aligns the hippocampal map during spatial reorientation. Curr. Biol. *27*, 309–317.
4. O'Keefe, J., and Dostrovsky, J. (1971). The hippocampus as a spatial map. Preliminary evidence from unit activity in the freely-moving rat. Brain Res. *34*, 171–175.
5. Olton, D.S., Branch, M., and Best, P.J. (1978). Spatial correlates of hippocampal unit activity. Exp. Neurol. *58*, 387–409.
6. Best, P.J., and Ranck, J.B., Jr. (1982). Reliability of the relationship between hippocampal unit activity and sensory-behavioral events in the rat. Exp. Neurol. *75*, 652–664.
7. Taube, J.S., Muller, R.U., and Ranck, J.B., Jr. (1990). Head-direction cells recorded from the postsubiculum in freely moving rats. I. Description and quantitative analysis. J. Neurosci. *10*, 420–435.
8. Sargolini, F., Fyhn, M., Hafting, T., McNaughton, B.L., Witter, M.P., Moser, M.-B., and Moser, E.I. (2006). Conjunctive representation of position, direction, and velocity in entorhinal cortex. Science *312*, 758–762.
9. Hafting, T., Fyhn, M., Molden, S., Moser, M.-B., and Moser, E.I. (2005). Microstructure of a spatial map in the entorhinal cortex. Nature *436*, 801–806.
10. Solstad, T., Boccara, C.N., Kropff, E., Moser, M.-B.B., and Moser, E.I. (2008). Representation of geometric borders in the entorhinal cortex. Science *322*, 1865–1868.
11. Kropff, E., Carmichael, J.E., Moser, M.-B., and Moser, E.I. (2015). Speed cells in the medial entorhinal cortex. Nature *523*, 419–424.
12. Sovrano, V.A., Bisazza, A., and Vallortigara, G. (2002). Modularity and spatial reorientation in a simple mind: encoding of geometric and nongeometric properties of a spatial environment by fish. Cognition *85*, B51–B59.
13. Sovrano, V.A., Bisazza, A., and Vallortigara, G. (2003). Modularity as a fish (Xenotoca eiseni) views it: conjoining geometric and nongeometric information for spatial reorientation. J. Exp. Psychol. Anim. Behav. Process. *29*, 199–210.
14. Vargas, J.P., López, J.C., Salas, C., and Thinus-Blanc, C. (2004). Encoding of geometric and featural spatial information by goldfish (Carassius auratus). J. Comp. Psychol. *118*, 206–216.
15. Sovrano, V.A., Bisazza, A., and Vallortigara, G. (2007). How fish do geometry in large and in small spaces. Anim. Cogn. *10*, 47–54.
16. Kelly, D.M., and Spetch, M.L. (2001). Pigeons encode relative geometry. J. Exp. Psychol. Anim. Behav. Process. *27*, 417–422.
17. Vallortigara, G., Zanforlin, M., and Pasti, G. (1990). Geometric modules in animals' spatial representations: a test with chicks (Gallus gallus domesticus). J. Comp. Psychol. *104*, 248–254.
18. Gouteux, S., Thinus-Blanc, C., and Vauclair, J. (2001). Rhesus monkeys use geometric and nongeometric information during a reorientation task. J. Exp. Psychol. Gen. *130*, 505–519.
19. Hermer, L., and Spelke, E. (1996). Modularity and development: the case of spatial reorientation. Cognition *61*, 195–232.
20. Winkler-Rhoades, N., Carey, S.C., and Spelke, E.S. (2013). Two-year-old children interpret abstract, purely geometric maps. Dev. Sci. *16*, 365–376.
21. Hermer, L., and Spelke, E.S. (1994). A geometric process for spatial reorientation in young children. Nature *370*, 57–59.
22. Kelley, D.M., and Spetch, M.L. (2004). Reorientation in a two-dimensional environment: II. Do pigeons (Columba livia) encode the featural and geometric properties of a two-dimensional schematic of a room? J. Comp. Psychol. *118*, 384–395.
23. Cheng, K., and Newcombe, N.S. (2005). Is there a geometric module for spatial orientation? Squaring theory and evidence. Psychon. Bull. Rev. *12*, 1–23.
24. Cheng, K., Huttenlocher, J., and Newcombe, N.S. (2013). 25 years of research on the use of geometry in spatial reorientation: a current theoretical perspective. Psychon. Bull. Rev. *20*, 1033–1054.
25. Julian, J.B., Keinath, A.T., Muzzio, I.A., and Epstein, R.A. (2015). Place recognition and heading retrieval are mediated by dissociable cognitive systems in mice. Proc. Natl. Acad. Sci. USA *112*, 6503–6508.
26. Marchette, S.A., Ryan, J., and Epstein, R.A. (2017). Schematic representations of local environmental space guide goal-directed navigation. Cognition *158*, 68–80.
27. Xu, Y., Regier, T., and Newcombe, N.S. (2015). An adaptive cue combination model of spatial reorientation. Cognition *163*, 55–66.
28. Ratliff, K.R., and Newcombe, N.S. (2008). Reorienting when cues conflict: evidence for an adaptive-combination view. Psychol. Sci. *19*, 1301–1307.
29. Packard, M.G., and McGaugh, J.L. (1996). Inactivation of hippocampus or caudate nucleus with lidocaine differentially affects expression of place and response learning. Neurobiol. Learn. Mem. *65*, 65–72.
30. Packard, M.G., and McGaugh, J.L. (1992). Double dissociation of fornix and caudate nucleus lesions on acquisition of two water maze tasks: further evidence for multiple memory systems. Behav. Neurosci. *106*, 439–446.

31. Mizumori, S.J.Y.Y., Yeshenko, O., Gill, K.M., and Davis, D.M. (2004). Parallel processing across neural systems: implications for a multiple memory system hypothesis. Neurobiol. Learn. Mem. *82*, 278–298.
32. McDonald, R.J., and White, N.M. (1993). A triple dissociation of memory systems: hippocampus, amygdala, and dorsal striatum. Behav. Neurosci. *107*, 3–22.
33. Byrne, P., Becker, S., and Burgess, N. (2007). Remembering the past and imagining the future: a neural model of spatial memory and imagery. Psychol. Rev. *114*, 340–375.
34. Wilber, A.A., Clark, B.J., Forster, T.C., Tatsuno, M., and McNaughton, B.L. (2014). Interaction of egocentric and world-centered reference frames in the rat posterior parietal cortex. J. Neurosci. *34*, 5431–5446.
35. Xu, Y., Regier, T., and Newcombe, N.S. (2017). An adaptive cue combination model of human spatial reorientation. Cognition *163*, 56–66.
36. Valerio, S., and Taube, J.S. (2012). Path integration: how the head direction signal maintains and corrects spatial orientation. Nat. Neurosci. *15*, 1445–1453.
37. van der Meer, M.A.A., Richmond, Z., Braga, R.M., Wood, E.R., and Dudchenko, P.A. (2010). Evidence for the use of an internal sense of direction in homing. Behav. Neurosci. *124*, 164–169.
38. Butler, W.N., Smith, K.S., van der Meer, M.A.A., and Taube, J.S. (2017). The head-direction signal plays a functional role as a neural compass during navigation. Curr. Biol. *27*, 1259–1267.
39. Dudchenko, P.A., and Taube, J.S. (1997). Correlation between head direction cell activity and spatial behavior on a radial arm maze. Behav. Neurosci. *111*, 3–19.
40. Taube, J.S., and Bassett, J.P. (2003). Persistent neural activity in head direction cells. Cereb. Cortex *13*, 1162–1172.
41. Winter, S.S., and Taube, J.S. (2014). Head direction cells: from generation to integration. In Space, Time and Memory in the Hippocampal Formation, D. Derdikman, and J.J. Knierim, eds. (Vienna: Springer), pp. 83–106.
42. Knight, R., Hayman, R., Lin Ginzberg, L., and Jeffery, K. (2011). Geometric cues influence head direction cells only weakly in nondisoriented rats. J. Neurosci. *31*, 15681–15692.
43. Clark, B.J., Harris, M.J., and Taube, J.S. (2012). Control of anterodorsal thalamic head direction cells by environmental boundaries: comparison with conflicting distal landmarks. Hippocampus *22*, 172–187.
44. Morris, R. (1984). Developments of a water-maze procedure for studying spatial learning in the rat. J. Neurosci. Methods *11*, 47–60.
45. Ratliff, K.R., and Newcombe, N.S. (2008). Is language necessary for human spatial reorientation? Reconsidering evidence from dual task paradigms. Cognit. Psychol. *56*, 142–163.
46. Twyman, A., Friedman, A., and Spetch, M.L. (2007). Penetrating the geometric module: catalyzing children's use of landmarks. Dev. Psychol. *43*, 1523–1530.

STAR★METHODS

KEY RESOURCES TABLE

REAGENT OR RESOURCE	SOURCE	IDENTIFIER
Chemicals		
PBS (10x)	Sigma-Aldrich	P5493-4L
Paraformaldehyde	Sigma-Aldrich	HT501128-4L
Buprenorphine	Vetmarket	0.3 mg/ml, 10 mL, http://www.vetmarket.co.il
Isoflurane	Vetmarket	http://www.vetmarket.co.il
Software and Algorithms		
MATLAB v2011b	MathWorks	https://www.mathworks.com/
Recording software: Cheetah v5.6	Neuralynx	http://neuralynx.com/
Spike sorting software	Neuralynx	SpikeSort3D
LabBook – documentation and actuator control software	Fellous lab website	http://amygdala.psychdept.arizona.edu/lab.html
Experimental Models: Organisms/Strains		
Rats: Long-Evans HsdBlue:LE	Harlan - Envigo	3BLU:LE01
Other		
Stereotaxic apparatus	David Kopf Instruments	Model #942
Lynx SX Recording platform	Neuralynx	http://neuralynx.com/
Gold pins	Neuralynx	large EIB Pins
Recording wires	California Fine Wire	Model:M283720 size: 17 μm, Platinum 10% Iridium
Head-stage tether	Neuralynx	HS-18
Head-stage connector	Omnetics	NPD-18-DD-GS
Electronic interface board (EIB)	Custom-built by Rogat Enterprises	N/A
Mircodrive	Custom-built by Rogat Enterprises	N/A
Drive assembly mount for EIB	Custom-built by Rogat Enterprises	N/A
Motorized feeders and rotation plate	Custom-built by Rogat Enterprises	N/A

CONTACT FOR REAGENT AND RESOURCE SHARING

Further information and requests for resources and reagents should be directed to and will be fulfilled by the Lead Contact, Dori Derdikman (derdik@technion.ac.il).

EXPERIMENTAL MODEL AND SUBJECT DETAILS

Subjects and surgery

Five adult male Long-Evans rats (healthy, drug naive, HsdBlue:LE strain, 500–700 g, 6-8 months old, not involved in previous procedures) were implanted with recording electrodes under isoflurane anesthesia and buprenorphine analgesia. Rats were implanted with microdrives (custom PCB and drive by Rogat, Carmiel, Israel, head-stage connector by Omnetics Connector Corporation, Minneapolis MN, USA) that contained four tetrodes (17-μm, Platinum 10% Iridium, California Wire Company), mounted on a moveable assembly for recording neuronal activity and local field potentials in the medial entorhinal cortex (0.3-0.5 mm anterior of transverse sinus; 4.5-4.6 mm ML; 2-2.4 mm DV). A ground screw was inserted into the frontal bone plate and attached by a wire to the microdrive during recording sessions. Rats were monitored for 1-2 weeks of recovery prior to recording, and maintained above 85% of their free-feeding weight. Rats were in a 12/12hr light/dark regime, dark period- 10:00-22:00. Rats were held in 46.2 × 40.3 × 40.4 cm cages with sawdust bedding. All experimental procedures were approved by the Animal Care and Use Committee of the Technion – Israel Institute of Technology.

METHOD DETAILS

Apparatus

The experimental arena consisted of an open-top wooden box, 60x120x60 cm, similar in dimensions to the one used by Cheng [1]. Four DC stepper motors controlled rotating feeders at the arena corners. Each feeder contained 15 wells baited with chocolate

sprinkles covered by a plastic lid, with a single hole facing the center of the arena, and enclosed with a wire mesh. This mesh was complete in 3 feeders, but perforated in 1 feeder, aligned to a single feeding well. This method prevented access to the feeding wells in all but the correct corner, while preserving similar olfactory, auditory, and visual cues originating from all feeders. A rotating plate at the center of the arena was used to disorient the rats, and a black PVC cylinder was used to restrain the rats on the central plate between trials.

Training protocol

Prior to training, rats were handled once a day for one week. The training protocol consisted of 8 stages: (1) Open-field training. Rats were trained to forage for a randomly placed food reward (chocolate sprinkles). This stage was repeated until full coverage of the arena was observed. (2) Food rewards were restricted to the top covers of the feeders, at the corners of the arena, and replaced each time the rat consumed the food, for 15 min. (3) Food rewards were restricted to a single feeder at a certain corner (randomized across days), activated to reveal subsequent rewards only after the rat stepped away from the baited corner. This stage was repeated until rats consumed 15 rewards within 15 min. (4) Additional food rewards were placed at the center of the arena each time the rat reached the goal location. Rats were trained to make repetitive trials between baited corners and central plates (non-rotating). This stage was repeated until rats maintained over 80% success for a first corner choice ratio. (5) A delay was introduced between food retrieval journeys to enable trial separation, by containing the rat inside a collapsible PVC cylinder for 30 s prior to the next foraging trial. (6) A slow rotation (5 rpm) of the central plate (cylinder floor) was introduced during all inter-trial periods inside a cylinder, for habituation to rotation and motor noise. (7) Periods of 5 consecutive fast rotations (12 rpm) of the central plate were randomly introduced during inter-trial periods. Once the corner choice success rate exceeded 85%, rats were implanted with micro-drives. (8) After recovery, rats were re-trained for stage 7, and transitioned to performing three behavioral sessions each day in an A–B–A′ experimental design: A 20 min open-field/random foraging session was recorded before and after each task session, to establish spatial tuning and stability of spatial activity of cells. Task sessions consisted of 15-45 trials, depending on individual rat performance - task sessions terminated once a rat showed signs of discomfort or stopped initiating new trials.

Behavioral task

Each trial began with a rat inside the cylinder at the center of the arena. Upon removal of the cylinder walls, rats located the correct corner and fed from its feeder. The rat was then returned to the center of the arena, where it was contained in the cylinder for 30 s. Disorientation was achieved by rotating the rat on a rubber-coated plate in the center of the arena at 12 rpm for 5 revolutions. During disorientation events, the opaque PVC cylinder walls prevented visual tracking of the correct corner. After each disorientation interval, the polarity of a DC motor turning the plate was inverted, changing the direction of rotation between disorientation events. Rats were not removed from the arena during recording sessions, and did not undergo the disorientation procedure in every trial. Task sessions consisted of 15-45 trials, and were terminated after 90 min, or once 45 trials were completed, or if a rat ceased to initiate new trials by returning to the center of the arena. Rats were not rewarded for making rotational errors (i.e., going to the incorrect 'rotational' corner), but were allowed to correct their choices and feed at the correct corner before returning to the central plate to start the next trial.

Controlling for external cues

We sought to minimize external cues, other than arena geometry, while reducing trial-to-trial variance and increasing environment ambiguity. We note that prior work showed that disorientation can enhance the salience of geometric cues for HD cell orientation [42,43]. Two white-noise speakers were suspended from the room ceiling, and the use of white noise doubled as a cue for task sessions versus open-field. Unified lighting was achieved by 8 evenly spaced DC LED lights, while a black curtain obstructed the rats' view of the room walls, and the experimenter walked in circles around the arena in random directions. On each recording day, the correct corner location was altered to maintain a hippocampal-dependent task [44]. "Correct corners" for each session were changed daily, and were chosen to match the tuning of the majority of HD cells for a given day, as recorded in the first open-field session (A). Animals that experience an environment under oriented conditions have been shown to apply the directional value of non-geometric cues to guide behavior and to continue using these cues after disorientation [45,46]. To mitigate this potentially confounding variable, the arena was cleaned before and after each session, and any feces were collected after each trial. If animals urinated in the arena, a paper towel was used to smear urine on all four corners. We exerted great effort to minimize non-geometric cues by removing, as much as we could, visual, auditory, and olfactory cues. While we could not guarantee full removal of all non-geometric cues, we believe this is not detrimental to the interpretation of our results and our drawing conclusions.

Data acquisition

All data were collected using the Digital Lynx SX data acquisition system (Neuralynx, Dublin, Ireland) at 32 KHz and Cheetah 5.6 software (Neuralynx). All signals were pre-processed with a bandpass filter of 600-6000 Hz. Single units were manually isolated into cell clusters using SpikeSort3D software (Neuralynx). Animal position was tracked using two LEDs mounted on the headstage, connected to the implanted microdrive. Tetrodes were lowered 50-100um per day until theta oscillations were observed in the local field potentials of a continuously recorded signal, and HD or grid cells were detected. Data were gathered from 59 recording sessions, and consisted of 163 HD cells, 54 grid cells, and 116 conjunctive- grid x HD cells. To reduce effects of noisy recordings, we included only

trials with score values above a threshold of ± 0.1 for a HD score and ± 0.05 for grid orientation score (see score calculation formulas below). Cells were divided into two groups for analysis: 158 HD cells with significant directional selectivity; and 170 putative grid cells with significant spatial selectivity (putative grid cells – the size of the arena precluded definite determination of grid cells). Some of the cells (n = 90) belonged to both groups (conjunctive grid X HD cells). To ensure that any neural correlations found had arisen from task-related behavior, our analysis only included spikes from trials with a positive task-engagement score. Hence, data were restricted to 1,334 trials, across 281 blocks.

Histology

Rats were perfused with PBS (Sigma-Aldrich) followed by 4% paraformaldehyde (Sigma-Aldrich). Brains were removed and stored in 4% paraformaldehyde for 2-3 days at 4°C, then transferred to PBS for 1-2 days. Brains were next placed in sucrose solutions of rising concentrations: 10%, 20% and 30% over a period of 5-7 days. Following fixation, brains were sliced into 30μm thick slices in a cryostat at −20°C. To identify tetrode trace, selected slices were treated with increasing gradients of ethanol solution to remove any fat in tissue, and then with decreasing gradients to rehydrate slice tissue. Finally, slices were stained with Cresyl violet to distinguish cell bodies.

QUANTIFICATION AND STATISTICAL ANALYSES

For analysis, we included only cells that demonstrated stable firing activity in both open-field recordings, or stability within the same recording in cases in which only a single recording was available. For grid cells, in order to test the stability of spatial firing patterns, each cell's spike train was randomly shifted in time (within the recording time) for 100 repetitions, to create a random distribution against which the correlation value of resulting rate maps from different open-field recordings could be compared. Cells that scored correlation values higher than 95/100 randomly generated values were classified as stable. All statitical analyses was cuncducted using MATLAB software. Only grid cells that fulfilled this criterion were included in the task analysis. Some of the cells that passed this spatial stability selection process displayed only few focal firing fields and could not be defintively assigned a grid-cell clasification, due to the inability of traditional gridness scores to capture the periodicity of firing fields in the confinements of a small arena (See Figure S4 for a distribution of gridnesss scores versus number of firing fields).

For HD cells, a similar procedure was carried out to test the significance of each cell's Rayleigh score— the cell's tendency to fire when the rat was faced in a certain direction. In addition to the directional significance test, only cells with a Rayleigh score of 0.3 or above were considered for analysis. For both HD cells and grid cells, trials in which the firing rate did not exceed 0.05 Hz were not included in the analysis. In addition, stability of the cells was required between the A and A' open-field sessions, before and after the task.

To estimate corner choice dynamics, we defined a distance threshold of 30 cm from the center of the arena (the diameter of the spinning plate) and a speed threshold of 15 cm/sec (about half of the full body length per second). For each trial, the time the rat first crossed the distance threshold was noted. Two behavioral classifiers were applied to the trial. The first classifier was based on a more "automatic" behavior, determined by (a) the corner closest to the location of the animal at the first local minima in the animal's speed (below the speed threshold), between the start of the trial and the rat's returning to the cylinder. This measure provides an immediate estimate of task performance (i.e., - corner choice); and was found to correlate better with brain activity of HD cells and grid cells, as described in this paper. The second classifier (b) was similar to (a) but with an aditional criterion: the first local minima after which speed did not rise above the threshold for at least 1 s (Figure S1A). This classifier indicated the rat's level of engagement in the task. As a rat could only initiate a new trial after consuming the reward at a goal location, we expected it to linger near the reward site when it was engaged in the task. To ensure that neural correlation arose from task-related behavior, we included in our analysis only trials with a positive task-engagement score. We note that the rat eventually reached the correct corner in almost every trial. In cases in which it made a rotational error, it corrected itself, sometimes reaching an erroneous corner a number of times, and then running to the correct corner. Thus, we considered the corner eventually reached as a measure of task engagement, and an indication that the rat was still trying to perform the task. Classified corner choices were assigned numerical values as a means of scoring behavior: +1 for correct, and −1 for rotational corner error. As with task performance scores, Near and Far errors were removed from the analysis, although behavioral results that examined these errrors can be found in Figure 1E, Figures S1A and S1B.

To ascertain that the measures of task performance and task engagment were similar to those expected in the task, we compared the results of the automatic classification to a blind manual classification of 5 of the videos of the rats (one from each rat). A Mann-Whitney test was used to test for difference of similiraity of classifications. The results are summarized in Figures S2A and S2B. The ratio of trials with identical behavioral classification, between manual and automatic scoring, was not significantly different than the ratio found when comparing manual scoring between two experimenters. Task engagement showed impaired corner choice after disorientation (Figure S1B), followed by a learning curve along the trials of a single block (Figure S1C). Task engagement scores reflected a high overall level of engagement in the task during recording sessions: in 85.6% of trials the rats' first stopping location was at either correct or rotational error corners.

For population level analysis of neural data, histograms were centered to align HD tuning curves to a common "zero" position of the main firing peak. PFD was calculated separately for each trial. To correlate activity of HD cells with grid cells and behavior, an HD score was formulated; PFD values of each trial were normalized to transition from absolute −180° to +180° off center from the

main tuning peak (PFD) to a relative −1 to +1 scale, in which +1 = PFD aligned with data from open-field sessions and −1 = aligned 180° away. The HD score was created using a transformation formula:

$$HD\ score = -\frac{|PFD|}{90} + 1$$

Similarly, correlations of grid cell rate maps were converted to an analogous grid orientation score, in which a score of +1 indicates a 1.0 correlation to an open-field recording rate map and a −1.0 correlation to a 180° rotated rate map of the same open-field recording; while a −1 score indicates the opposite: a −1.0 correlation to an open-field recording rate map and +1.0 correlation to a 180° rotated rate map of the same open-field recording. The grid orientation score was created using a transformation formula:

$$Grid\ orientation\ score = \frac{correlation\ to\ openfield - correlation\ to\ rotated\ openfield}{2}$$

The normalization of HD, grid orientation and behavior outputs to a unified scale facilitated comparisons across neural and behavioral data of individual trials. By representing both behavioral and neural parameters on a common scale, it was easier to visualize the orientation state of different functional cell types in a single recording, on a trial by trial basis. Additionally, we were able to track changes that resulted from disorientation events. Using this unified scale, we traced the activity patterns of simultaneously recorded cells, and extracted population vectors of activity for HD cells and grid cells, as well as the behavioral outcome.

For correlation of neural activity to behavior in trials, the probability of correct choice was calaculated with or without considering head-direction and grid population vectors in past trials. Significance of results was tested using the chi-square test for the difference between positive and negative population vector values in current and previous trials, df = 2 (Figure 4). Similarly, for trial-blocks, significance of results was tested using chi-square test for the difference between positive and negative population vector values in each frequency of past instances, df = 2 (Figure S3).

Stability measurement: permutation test

To measure within-block stability of behavior, HD or grid population vectors, we employed the following procedure: for each recording session, we permutated the values of each trial within the same session and compared the values taken from the same block against those of the 1,000 repetitions of randomly permutated values across all blocks within a given recording session (H_0, the proportion of same sign trial values across blocks does not differ from those within blocks.). A stability score (S) was calculated as the absolute difference between the number of positive and negative trial scores within a block divided by the sum of all trials. P denotes the number of positive trials; N denotes the number of negative trials. S was considered significant if observed values were higher than 990/1,000 repetitions of permutations of trials across blocks.

$$S = \frac{\sum |P - N|}{\sum (P + N)}$$

DATA AND SOFTWARE AVAILABILITY

Data and custom MATLAB codes used to generate all analyses are available from the Lead Contact upon request.